www.elsevier.com/locate/jbiomech

Differential responses of induced pluripotent stem cell-derived cardiomyocytes to anisotropic strain depends on disease status

Young Wook Chun, David E. Voyles, Rutwik Rath, Lucas H. Hofmeister, Timothy C. Boire, Henry Wilcox, Jae Han Lee, Leon M. Bellan, Charles C. Hong, Hak-Joon Sung

PII: S0021-9290(15)00522-9
DOI: http://dx.doi.org/10.1016/j.jbiomech.2015.09.028
Reference: BM7336

To appear in: *Journal of Biomechanics*

Received date: 11 June 2015
Revised date: 10 September 2015
Accepted date: 24 September 2015

Cite this article as: Young Wook Chun, David E. Voyles, Rutwik Rath, Lucas H. Hofmeister, Timothy C. Boire, Henry Wilcox, Jae Han Lee, Leon M. Bellan Charles C. Hong and Hak-Joon Sung, Differential responses of induce pluripotent stem cell-derived cardiomyocytes to anisotropic strain depends o disease status, *Journal of Biomechanics* http://dx.doi.org/10.1016/j.jbiomech.2015.09.028

Differential responses of induced pluripotent stem cell-derived cardiomyocytes to anisotropic strain depends on disease status

Young Wook Chun[1,2], David E. Voyles[1], Rutwik Rath[1], Lucas H. Hofmeister[1], Timothy C. Boire[1], Henry Wilcox[3], Jae Han Lee[1], Leon M. Bellan[1,4], Charles C. Hong[2,5*], and Hak-Joon Sung[1,2*].

Affiliations: [1] Department of Biomedical Engineering, [2] Division of Cardiovascular Medicine, Vanderbilt University, Nashville, TN 37235

[3] Department of Biochemistry and Cellular and Molecular Biology, University of Tennessee, Knoxville, TN 37996

[4] Department of Mechanical Engineering, Vanderbilt University, Nashville, TN 37235

[5]Research Medicine, Veterans Affairs TVHS, Nashville, TN 37212

*Co-correspondence should be addressed to:

Hak-Joon Sung, Ph.D.
E-mail: hak-joon.sung@vanderbilt.edu
VU Station B #351631, Nashville, TN 37235
Tel: 615/322-6986/ Fax: 615/343-7919

Charles C. Hong, MD, Ph.D
E-mail: charles.c.hong@vanderbilt.edu
Associate Professor of Cardiovascular Medicine,
Pharmacology, and Cell and Developmental Biology
Vanderbilt University School of Medicine
Nashville, TN 37232
Office: (615) 936-7032; Fax: (615) 936-1872; Lab: (615) 322-5098

Key words: anisotropic strain; dilated cardiomyopathy; iPSC; cardiac maturation; cell-cell interaction.

Word counts: 3592 words (~ 12 pages)

Abstract

Primary dilated cardiomyopathy (DCM) is a non-ischemic heart disease with impaired pumping function of the heart. In this study, we used human induced pluripotent stem cell-derived cardiomyocytes (iPSC-CMs) from a healthy volunteer and a primary DCM patient to investigate the impact of DCM on iPSC-CMs' responses to different types of anisotropic strain. A bioreactor system was established that generates cardiac-mimetic forces of 150 kPa at 5% anisotropic cyclic strain and 1 Hz frequency. After confirming cardiac induction of the iPSCs, it was determined that fibronectin was favorable to other extracellular matrix protein coatings (gelatin, laminin, vitronectin) in terms of viable cell area and density, and was therefore selected as the coating for further study. When iPSC-CMs were exposed to three strain conditions (no strain, 5% static strain, and 5% cyclic strain), the static strain elicited significant induction of sarcomere components in comparison to other strain conditions. However, this induction occurred only in iPSC-CMs from a healthy volunteer ("control iPSC-CMs"), not in iPSC-CMs from the DCM patient ("DCM iPSC-CMs"). The donor type also significantly influenced gene expressions of cell-cell and cell-matrix interaction markers in response to the strain conditions. Gene expression of connexin-43 (cell-cell interaction) had a higher fold change in healthy versus diseased iPSC-CMs under static and cyclic strain, as opposed to integrins α-5 and α-10 (cell-matrix interaction). In summary, our iPSC-CM-based study to model the effects of different strain conditions suggests that intrinsic, genetic-based differences in the cardiomyocyte responses to strain may influence disease manifestation *in vivo*.

1. Introduction

Primary dilated cardiomyopathy (DCM) is a leading cause of heart failure, second only to ischemic heart disease (Sehnert et al., 2002; Sun et al., 2012). A common pathophysiology of primary DCM is thought to involve compromised contractility of cardiomyocytes (CMs), leading to impaired

systolic function of the heart. As heart failure progresses, the ventricles remodel, dilate and their walls thin (Marian and Roberts, 1994; Morita et al., 2005; Willott et al., 2010). Although primary DCM is classically considered idiopathic, a significant fraction of the cases is now known to involve specific gene mutations affecting the CM structure and function (Herman et al., 2012).

In the healthy adult heart, CMs are characterized by their interactions between neighboring cells as well as the surrounding matrix. In CMs, gap junctions are responsible for mechanical and electrical coupling between cells and action potential transmission (Christoforou et al., 2013; Simon et al., 1998; Willecke et al., 2002). In particular, among the connexin gene family that is responsible for development of gap junction in CMs (Christoforou et al., 2013; Palatinus et al., 2012), connexin-43 (Cx43) is the most abundant in the heart and ventricular muscle, and low levels of its protein expression have been previously associated with ventricular arrhythmia in DCM patients (Kitamura et al., 2002; Severs et al., 2008). On the other hand, cell-matrix interactions, mediated by integrins, are also critical for the maturation and function of CMs. Of the 16 α-subunits in mammalian cells, only seven subunits, α1, α3, α5, α6, α7, α9, and α10, are expressed in CMs (Ross and Borg, 2001). Fetal and neonatal CMs contain the α1, α3, α5 subunits, whereas healthy adult CMs lack α1 and α5 subunits (Terracio et al., 1991). This suggests that these subunits can be used as markers of CM immaturity.

In order to better elucidate and ultimately regulate the cellular mechanisms that cause DCM, *in vitro* models are needed that employ a cell source recapitulating the behavior of diseased CMs. Previous studies have shown that iPSCs raised from healthy and diseased donors can be used to generate *in vitro* models of DCM in iPSC-derived CMs (iPSC-CMs) (Rajala et al., 2011; Schwartz et al., 1995). In this study, CMs were derived from iPSCs of both a healthy donor and a 7 month old male patient with congenital DCM, a rare but fatal disorder. This DCM patient has no family history of the disease and its etiology is also unknown. CMs derived from iPSCs of both cell sources were exposed to three different conditions of anisotropic

strain (no strain, 5% static strain, and 5% cyclic strain) to study how these different culture conditions influence the structure and function of CMs by altering cell-cell and cell-matrix interactions.

2. Materials and Methods

2.1 Reprogramming, Passaging, and Cardiac Differentiation of iPSCs. Human skin fibroblasts were obtained from either a healthy donor or a DCM patient (7 month old male) at the Vanderbilt University Medical Center following appropriate consent under the guideline of an approved IRB protocol (Vanderbilt #080369). Cells from only one patient with congenital DCM were obtained due to the rarity of this disorder. The patient has no family history of DCM and its etiology is unknown. Human iPSC lines were reprogrammed from skin fibroblasts by established methods (Aboud et al., 2014a; Okita et al., 2011; Wang et al., 2015; Yang et al., 2014). Specifically, vector pEP4EO2SCK2MEN2L (OCT4/SOX2/KLF4/MYC/NANOG/LIN28) and pEP4EO2SET2K (OCT4/SOX2/LT/KLF4) were co-transfected into 1.0×10^6 human skin fibroblasts via nucleofection (VPD-1001 with program U-23, Amaxa, MD). Transfected fibroblasts were plated directly to Matrigel-coated dishes in fibroblast medium. On day one post-transfection, fibroblast medium were replaced with reprogramming medium consisting of DMEM/F12 culture medium supplemented with N-2 supplement (Invitrogen), B27 (Invitrogen), 0.1 mM nonessential amino acids, 1 mM GlutaMAX, 0.1 mM β-mercaptoethanol, PD0325901 (P, 0.5 mM), CHIR99021(C, 3 mM), A-83- 01(A, 0.5 mM) (all from Stemgent, San Diego, CA), hLIF (L, 1000 U/ml, Millipore) and HA-100 (H, 10 mM). Culture media were refreshed every other day. On day 13 post-transfection, the transfected cells were cultured with mTeSR1 to expand iPSCs.

These iPSC lines were cultured and maintained following the previously published methods (Aboud et al., 2012; Aboud et al., 2014b; Okita et al., 2011). Upon 80~90% confluence, cardiac

induction of these cells was conducted by the "Matrigel sandwich" method as described previously (Zhang et al., 2012). The cardiac differentiated cells were maintained in RPMI/B27 without insulin until day 10-11. The culture media was then changed every other day for one week with RPMI/B27 media containing neither insulin nor glucose. The iPSC-CMs were maintained in this RPMI/B-27 supplement until after cardiac differentiation on day 30.

Characterization of iPSC-CMs. Cardiac differentiation of iPSC-CMs was evaluated by Flow Cytometry (FACS, BD FACSAria III). ~10^6 cells were fixed in 4% paraformaldehyde and permeabilized by a FACS buffer with 0.1% saponin. Troponin T mouse monoclonal antibodies (Santa Cruz Biotechnology) diluted in FACS buffer (1:50) as primary antibodies and the primary IgG isotype (Donkey anti-mouse, Invitrogen) as secondary antibodies were used for FACS analysis. The resulting data were analyzed using FlowJo v8.5.2.

For immunostaining, fixed, permeabilized cells were blocked and treated with Troponin T mouse monoclonal antibodies (Santa Cruz Biotechnology) and α-actinin mouse monoclonal antibodies (Sigma), followed by incubation with with IgG secondary antibodies and counter staining with DAPI. Slides were viewed with a confocal microscope (Olympus FV-1000) and the image analysis was done with NIS-Elements BR3.0 software.

2.2 Fabrication of PDMS devices. A silicone elastomer was created using a 1:10 ratio of catalyst to elastomer base by mass (Sylgard 184, Dow Corning). The resulting poly-dimethyl siloxane (PDMS) solution was poured into a pre-fabricated mold and degassed under vacuum for 15 minutes to remove air bubbles. Large rectangular glass coverslips were clamped onto the PDMS molds to provide a flat surface and the molds were cured overnight at 70°C. The following day, PDMS molds (overall thickness of 1/8 of an inch) were removed and placed in 70% ethanol for several days to remove any unreacted catalyst and ultimately placed in a 90°C oven for 30 minutes to evaporate the ethanol. The device contains a cell

culture channel with two wells measuring 10 mm x 10 mm x 1 mm (L x W x H), in which the cells were seeded and cultured. A fiberglass embedding technique was used to integrate actuator harnesses into the stretcher device, allowing easy loading of the PDMS device onto the bioreactor system. The elastic modulus of the device was measured in a parallel plate configuration on a rheometer (RA2000, TA Instrument) in oscillation mode with a frequency of 1 Hz and 5% strain at 37°C.

2.3 Bioreactor system: In order to control the strain dynamics on the PDMS device, a design integrating a fixed point and an opposing micro-positioning linear actuator were chosen. The actuators used in the bioreactor system are Physik Instrumente M-235.5DD high power direct drive DC actuators with a ballscrew driving mechanism (Physik Instrumente, GmbH). The actuators have a total travel length of 50 mm. Ballscrew actuators were chosen to reduce the backlash when performing cyclic motion. Direct drive DC-driven linear actuators were chosen to achieve the high speeds and accelerations necessary for 1 Hz cyclic motion akin to human physiology and produce smooth displacement curves. In addition, these actuators provide forces of over 120 N and incremental motion of 0.5 μm with 0.5 μm repeatability. The actuators are equipped with rotary encoders for feedback during the control process. Control of the bioreactor system was achieved through a PCI bus card integrated into the control computer and using Labview. Before bioreactor operation, the actuators were first referenced to non-contact hall-effect limit switches and then moved into position to load the PDMS devices to the system. A MATLAB program was used to write the motion profile instructions for the actuators and was capable of writing any arbitrary waveform to a set of motion instructions for the actuators. Additional parameters were tested, such as 1, 5, 7, and 10% strain (data not shown), frequency of strain (0.5 to 2 Hz using 0.5 increments (Figure 1), and length of exposure to strain was also extended past 48 hours (data not shown). These parameters tested were based on previous works (Clements et al., 1997; Govoni et al., 2013b; Hoit, 2011; Nguyen et al., 2013b; Shimko and Claycomb, 2008a; Yamamoto et al., 2001).

2.4 Protein coating. Clean and dry PDMS molds were placed in Harrick Plasma PDC-002 under vacuum. The unit was set to high and the samples were then treated with plasma for 90 seconds. The molds were removed and immediately coated with a pre-mixed solution of an extracellular matrix protein (5μg/cm^2) in serum-free medium. Four protein coatings were tested; gelatin as it increases beating behavior and functions of cardiomyocytes (Koch-Schneidemann et al., 1994; Miskon et al., 2009), laminin as it improves cell attachment of adult cardiomyocytes (Koch-Schneidemann et al., 1994), fibronectin as it enhances the functions of cardiomyocytes derived from stem cells (Burridge et al., 2014; Gandaglia et al., 2012), and vitronectin because it increases the adhesion of cardiomyocytes (Braam et al., 2008; Michel, 2003). The resulting samples were covered with aluminum foil and left overnight on a shaker plate at 4°C prior to seeding cells.

2.5 Bioreactor culture. iPSC-CMs were cultured on Matrigel for 30 days after cardiac induction and seeded onto PDMS devices for 24 hours to allow for cell attachment. Cell-seeded PDMS stretching devices were mounted on the custom-built cyclic bioreactor and placed in an incubator at 37°C and 5% CO_2. Samples were cyclically stretched at 1 Hz, 5% length based strain for 48 hours(Clements et al., 1997; Govoni et al., 2013a; Hoit, 2011; Nguyen et al., 2013a; Ruan et al., 2015; Shimko and Claycomb, 2008b; Yamamoto et al., 2001). Static controls were set up in a similar fashion and subject to 5% strain. No-strain controls were placed in the incubator and not subjected to any strain (Chien et al., 2008; Gwak et al., 2008). Samples were removed after 48 hours and prepared for specified endpoint assays.

2.6 Characterization of iPSC-CM viability and morphology. Cells on PDMS devices were stained with a live/dead mammalian assay (Life-Tech) according to the manufacturer's protocol. A Nikon Eclipse Ti inverted fluorescence microscope was used to image cells on the PDMS devices. For cell morphological analysis, images were imported into ImageJ (NIH, Bethesda, MA) and analyzed for cell area and density.

2.7 Analysis of gene expression by qRT-PCR. RNA was first extracted using Trizol (Invitrogen) and the RNeasy Mini Kit. cDNA was synthesized using the iScipt cDNA synthesis kit (Bio-Rad) and run for qRT-PCR using a thermocycler (Bio-Rad S1000^{TM}) with Platinum$^{®}$ Supermix (Life Technologies). The temperature cycle used for PCR went as follows: hot start for 3 minutes at 94ºC; denaturation for 30 seconds at 94ºC; annealing for 30 seconds; and extension for 1 minute at 72 ºC. GAPDH was used as a house keeping gene.

2.8 Analysis of Immunofluorescence staining. Fixed cells were permeabilized in PBS with 0.2% Triton X-100 and blocked overnight in PBS, followed by treatment with either primary donkey anti-cTNT antibodies or primary mouse anti-MLC-2v antibodies (both diluted to 1:200 in PBS). Samples were then incubated with either secondary donkey anti-goat Cy3-conjugated antibodies or secondary goat anti-mouse FITC conjugated antibodies (Abcam) (both diluted to 1:200 in PBS), followed by counterstaining of nuclei with Hoechst. Images of the cells were taken with a Nikon Eclipse Ti inverted fluorescence microscope, and all images were imported into ImageJ (NIH) for measurements of average fluorescence intensity per cell.

2.9 Statistical Analysis. Prism 5 Software was used for data analysis. All results are reported as the mean ± SEM. Unless otherwise noted, N=4 for biological replicates where the data was analyzed by two-way analysis of variance (ANOVA). The Bonferroni post hoc test was used for comparison between groups, and one-way ANOVA was used for analysis of unrelated groups. A value of $p<0.05$ was considered to be statistically significant.

3. Results

3.1 Bioreactor device characterization. A bioreactor was designed to produce anisotropic strain on iPSC-CMs in a controlled manner by operating two computer-programmable, compact micro-positioning stage linear actuators that can provide static or cyclic strains (See Fig. 1A, Videos S1, and

the method section for details). In order to verify that the PDMS device used with the bioreactor system accurately mimicked the cardiac environment, the stiffness (Young's modulus) of the device was measured. The ultimate loading program (5% strain, 1 Hz, 48 hour culture) was determined based on the constraint that the force and cycle experienced by the cells stay within physiological cardiac range (150 kPa, 1 Hz). This modulus was measured to be approximately 150 kPa, which compares well with that of the adult human myocardium (Bhana et al., 2010; Engelmayr et al., 2008b; Forte et al., 2008; Jawad et al., 2008) (Fig. 1B).

3.2 Confirmation of cardiac induction of iPSC derived from healthy and DCM donors. Directed differentiation of iPSCs derived from both healthy and DCM donors, outlined in Figs. 2A and 2B, successfully yielded iPSC-CMs. Visual inspection of the iPSC-CMs 10-13 days after differentiation showed both iPSC-CMs formed beating sheets of cells. Flow cytometry analysis demonstrated 90-95% of both cell types were positive for troponin T at 15 days post differentiation (Fig. 2A), which was confirmed by clear visualization of cardiac α-actinin and troponin T expression in both cell types using immunostaining (Fig. 2B).

3.3 Effects of ECM Coating and Varying Strain Conditions on Cell Viability, Area, and Density. To determine an optimal extracellular matrix type for coating of the stretcher, PDMS devices were coated with gelatin, laminin, vitronectin, or fibronectin. Healthy iPSC-CMs were seeded on the PDMS devices that were either unstrained or exposed to 5% static strain, and 5% cyclic strain. Cell viability (Fig. 3C), viable cell area (Fig. 2D), and cell density (Fig. 2E) results show significant differences between the types of coating. There was a significant decrease ($p<0.05$) in cell viability of unstrained iPSC-CMs on a vitronectin coat. No other significant differences were observed between the groups. Under all three strain conditions, cells placed on fibronectin presented the largest amounts of viable cell area. Cyclic strain data showed that while there was a significant increase ($P<0.05$) in viable cell density of cells on

gelatin compared to laminin and vitronectin, those plated on fibronectin showed the largest amounts of viable cell density ($P<0.001$) compared to the other three groups. These results suggest fibronectin as the best coating material among the tested ones for further experiments.

3.4 Expression of Cardiac Markers. TNNT2 is the gene that codes a sarcomeric cardiac protein, cardiac troponin T (cTNT), and Myosin Light Chain 2 Gene (MYL2) encodes MLC-2v protein. PCR analysis of TNNT2 and MYL2 expression (Fig. 3A-B) showed that under static strain, the two genes were expressed significantly more ($P<0.05$) in healthy CMs compared to diseased CMs. The expression levels of these genes were highest under static strain among all the test conditions. There were no significant differences in the expression of these two genes between healthy and diseased CMs when unstrained and exposed to cyclic strain. There were also no significant differences in the express of TNN2 between diseased CMs subject to different strain types, but in diseased CMs, static and cyclic strain degreased MYL2 expression significantly ($P<0.05$) compared to no strain, indicating that DCM iPSC-CMs may not be healthy enough to exert positive responses to the strain conditions.

Protein expression of cTNT and MLC-2v (Fig. 3 C-D) indicate that under static strain, these two proteins were expressed significantly more in healthy CMs compared to diseased CMs ($P<0.05$), which are consistent with the results of gene expression (Fig. 3A-B). There were no significant differences in protein expression of cTNT and MLC-2v between healthy and DCM iPSC-CMs when exposed to cyclic and no strain.

3.5 Cell-Cell and Cell-Matrix Interaction. The difference in protein expression of cTNT between healthy and DCM iPSC-CMs under the static strain condition was confirmed visually by immunostaining in Fig. 4A. Moreover, healthy iPSC-CMs showed aggregated cell clusters over the culture area, which was not seen in DCM iPSC-CMs. This difference indicates that altered cell-cell and cell-matrix interactions of healthy versus diseased iPSC-CMs might play a role in regulating their

cardiac structure and function. Therefore, gene expression levels of connexin-43 (cell-cell interaction) and integrins α5 and α10 (cell-matrix interaction) were examined by RT-PCR (Maitra et al., 2000; Palatinus et al., 2012). The three strain conditions showed 2.4-17.3 ratio of healthy to disease (H:D) connexin-43 expression (>1) (Fig. 4B), indicating an enhanced cell-cell interaction in healthy over DCM iPSC-CMs. On the other hand, expression of integrins α5 and α10 showed 0.07-0.64 H:D ratio (< 1), indicating an enhanced cell-matrix interaction in the diseased over healthy cells under the three strain conditions (Fig. 4C-D). While all strain groups show a substantial H:D ratio change between the expression of connexin-43 and both integrin subunits, the most notable changes are observed in the static condition. Cells exposed to cyclic strain also showed a relatively large change in H:D value between Cx43 and the integrin subunits, while a much smaller difference was observed in those that experienced no strain. Considering the fact that the H:D ratios of integrins α5 and α10 expression are similar for the three strain conditions, these results suggest the enhanced cell-cell interaction under the static and cyclic strain conditions as a critical aspect in maintaining cardiac structure and function of healthy iPSC-CMs over diseased cells.

4. Discussion

The goal of this study is to determine effects of genetic backgrounds carried from healthy and DCM patients on iPSC responses to anisotropic mechanical strain. In particular, the causative roles of DCM and mechanostimulation in expression of sarcomere structure and cell-cell/cell-matrix interaction markers were investigated. Either healthy or DCM iPSC-CMs we used in this study were isolated on day 30 after cardiac differentiation in order to keep identical maturity for all experiments. Additionally, the metabolic selection method was used for purifying CMs in the iPSC-derived cell population. It was expected that these minimized the variations resulted from each derivative.

Our study indicates that healthy and DCM iPSC-CMs show selective responses to different types of strain. It was found that local increases in stationary mechanical strain (~ 150 kPa) might help maintenance of cardiac structure and function of healthy iPSC-CMs because this values is similar to the range of the adult human myocardium (Engelmayr et al., 2008b; Forte et al., 2008; Jawad et al., 2008). However, this effect was not the same for DCM iPSC-CMs, most likely due to an altered genetic background. Results from this study suggest the dominant role of cell-cell interaction in driving the healthy iPSC-CM phenotype. In the analysis of matrix coatings, fibronectin proved to be the most suitable for this experiment in terms of viable cell area and cell density.

The measured Young's modulus value of PDMS device (~150 kPa) matches the stiffness values in the previously studied cardiac tissue models, and native rat myocardium has a Young's modulus in the range of 10 to 150 kPa (Bhana et al., 2010; Engelmayr et al., 2008a; Jawad et al., 2007). This suggests that the fabricated PDMS devices are able to create a mechanical environment similar to that of heart tissue. Static strain seemed to promote the healthy phenotype of iPSC-CMs, as evidenced by increased expression of genes and proteins associated with cardiac structure and function. Studies with mouse models have demonstrated that cTNT deficient CMs failed to assemble sarcomere structures from thick and thin filaments and were not able to produce heartbeats (Ameen et al., 2008). Higher expression of this protein in healthy iPSC-CMs under static conditions indicates a preferential differentiation toward a healthier CM phenotype with an overall increase in contractile function of the heart. DCM iPSC-CMs, on the other hand, did not respond to static strain in the same way that healthy iPSC-CMs did. MLC2 expression is also related to contractility of the heart, as well as thick-filament stabilization. The increased expression of MLC2 gene and protein under healthy, static conditions can explain a critical symptom of DCM, most notably a diminished systolic function accompanied by an inability to generate the necessary contractile force. Therefore, this result supports the idea that CM structure and

function are affected by a pathological status (altering cellular mechanism) related to DCM (Marian and Roberts, 1994; Morita et al., 2005; Willott et al., 2010). A previous study reported reduced beating rates and contractility with altered sarcomere structures in iPSC-CMs derived from DCM patients (Sun et al., 2012). Our study provides additional insight into differences in cardiac-specific structural organization and cell-cell/cell-matrix interactions between normal and DCM iPSC CMs in response to different strain types.

Next, the effects of DCM on cell-matrix and cell-cell interactions under the three types of strain were studied. Connexin-43 expression, the principle protein in gap junction interactions, was much higher in healthy iPSC-CMs than in DCM iPSC-CMs in all three stretching conditions. Reduction in Cx43 expression accompanies human ventricular disease and correlates with arrhythmic changes and contractile dysfunction in animal models (Severs et al., 2008). Cx43 expression is expected to decrease as lowered cell-cell interaction results in diminished electrical and mechanical coupling and thus a less cohesive and contractile tissue. DCM cells, suffering from the inability to generate an adequate contractile and uniform force, show a greatly reduced expression of this vital protein. In contrast, expression of specific cell-matrix promoting proteins (integrins α5 and α10) was significantly higher in iPSC-CMs derived from DCM patients. In fetal CMs, integrins α5 expression increases to improve cell attachment to ECM components such as collagen type I and fibronectin, whereas in adult CMs, its decreased expression results in reduced production of fibronectin receptors (Maitra et al., 2000). This result indicates that DCM-derived CMs may have more cell-matrix interactive, fetal phenotypes as evidenced by the increased expression of ITGA5.

Future studies will aim to further elucidate the effects of static strain on cardiac phenotype and cell-cell communication following damage from dilated cardiomyopathy using electrophysiological

tools. Understanding the maturation mechanism of DCM iPSC-CMs at molecular, cellular, and physiological levels will ultimately lead to future development of DCM patient-specific cell therapy.

The conflict of interest statement

The authors declare no conflicts of interest, financial or otherwise.

Acknowledgements

This research work was funded and supported by NIH R01HL104040, NIH UH2 TR000491, NIH R01ES010563, NIH R01ES016931, 1R01 NS078289, VA Merit 101BX000771, NSF CAREER CBET 1056046, the National Center for Research Resources Grant UL1 RR024975 and the National Center for Advancing Translational Sciences Grant UL1 TR000445. Polymer characterization was conducted through the use of the core facilities of the Vanderbilt Institute of Nanoscale Sciences and Engineering (VINSE), which was supported by NSF EPS 1004083.

References

Aboud, A.A., Tidball, A.M., Kumar, K.K., Diana Neely, M., Han, B., Ess, K.C., Hong, C.C., Erikson, K.M., Hedera, P., Bowman, A.B., 2014a. PARK2 patient neuroprogenitors show increased mitochondrial sensitivity to copper. Neurobiol Dis.

Aboud, A.A., Tidball, A.M., Kumar, K.K., Neely, M.D., Ess, K.C., Erikson, K.M., Bowman, A.B., 2012. Genetic risk for Parkinson's disease correlates with alterations in neuronal manganese sensitivity between two human subjects. Neurotoxicology 33, 1443-1449.

Aboud, A.A., Tidball, A.M., Kumar, K.K., Neely, M.D., Han, B., Ess, K.C., Hong, C.C., Erikson, K.M., Hedera, P., Bowman, A.B., 2014b. PARK2 patient neuroprogenitors show increased mitochondrial sensitivity to copper. Neurobiology of disease 73c, 204-212.

Ameen, C., Strehl, R., Bjorquist, P., Lindahl, A., Hyllner, J., Sartipy, P., 2008. Human embryonic stem cells: current technologies and emerging industrial applications. Critical reviews in oncology/hematology 65, 54-80.

Bhana, B., Iyer, R.K., Chen, W.L., Zhao, R., Sider, K.L., Likhitpanichkul, M., Simmons, C.A., Radisic, M., 2010. Influence of substrate stiffness on the phenotype of heart cells. Biotechnology and bioengineering 105, 1148-1160.

Braam, S.R., Zeinstra, L., Litjens, S., Ward-van Oostwaard, D., van den Brink, S., van Laake, L., Lebrin, F., Kats, P., Hochstenbach, R., Passier, R., Sonnenberg, A., Mummery, C.L., 2008. Recombinant vitronectin is a functionally defined substrate that supports human embryonic stem cell self-renewal via alphavbeta5 integrin. Stem Cells 26, 2257-2265.

Burridge, P.W., Matsa, E., Shukla, P., Lin, Z.C., Churko, J.M., Ebert, A.D., Lan, F., Diecke, S., Huber, B., Mordwinkin, N.M., Plews, J.R., Abilez, O.J., Cui, B., Gold, J.D., Wu, J.C., 2014. Chemically defined generation of human cardiomyocytes. Nat Methods 11, 855-860.

Chien, K.R., Domian, I.J., Parker, K.K., 2008. Cardiogenesis and the Complex Biology of Regenerative Cardiovascular Medicine. Science 322, 1494-1497.

Christoforou, N., Liau, B., Chakraborty, S., Chellapan, M., Bursac, N., Leong, K.W., 2013. Induced pluripotent stem cell-derived cardiac progenitors differentiate to cardiomyocytes and form biosynthetic tissues. PloS one 8, e65963.

Clements, M.L., Banes, A.J., Faber, J.E., 1997. Effect of Mechanical Loading on Vascular α1D- and α1B-Adrenergic Receptor Expression. Hypertension 29, 1156-1164.

Engelmayr, G.C., Cheng, M., Bettinger, C.J., Borenstein, J.T., Langer, R., Freed, L.E., 2008a. Accordion-Like Honeycombs for Tissue Engineering of Cardiac Anisotropy. Nat Mater 7, 1003-1010.

Engelmayr, G.C., Jr., Cheng, M., Bettinger, C.J., Borenstein, J.T., Langer, R., Freed, L.E., 2008b. Accordion-like honeycombs for tissue engineering of cardiac anisotropy. Nat Mater 7, 1003-1010.

Forte, G., Carotenuto, F., Pagliari, F., Pagliari, S., Cossa, P., Fiaccavento, R., Ahluwalia, A., Vozzi, G., Vinci, B., Serafino, A., Rinaldi, A., Traversa, E., Carosella, L., Minieri, M., Di Nardo, P., 2008. Criticality of the biological and physical stimuli array inducing resident cardiac stem cell determination. Stem Cells 26, 2093-2103.

Gandaglia, A., Huerta-Cantillo, R., Comisso, M., Danesin, R., Ghezzo, F., Naso, F., Gastaldello, A., Schittullo, E., Buratto, E., Spina, M., Gerosa, G., Dettin, M., 2012. Cardiomyocytes in vitro adhesion is actively influenced by biomimetic synthetic peptides for cardiac tissue engineering. Tissue Eng Part A 18, 725-736.

Govoni, M., Muscari, C., Guarnieri, C., Giordano, E., 2013a. Mechanostimulation protocols for cardiac tissue engineering. BioMed research international 2013, 918640.

Govoni, M., Muscari, C., Guarnieri, C., Giordano, E., 2013b. Mechanostimulation Protocols for Cardiac Tissue Engineering. BioMed Research International 2013, 918640.

Gwak, S.J., Bhang, S.H., Kim, I.K., Kim, S.S., Cho, S.W., Jeon, O., Yoo, K.J., Putnam, A.J., Kim, B.S., 2008. The effect of cyclic strain on embryonic stem cell-derived cardiomyocytes. Biomaterials 29, 844-856.

Herman, D.S., Lam, L., Taylor, M.R.G., Wang, L., Teekakirikul, P., Christodoulou, D., Conner, L., DePalma, S.R., McDonough, B., Sparks, E., Teodorescu, D.L., Cirino, A.L., Banner, N.R., Pennell, D.J., Graw, S., Merlo, M., Di Lenarda, A., Sinagra, G., Bos, J.M., Ackerman, M.J., Mitchell, R.N., Murry, C.E., Lakdawala, N.K., Ho, C.Y., Barton, P.J.R., Cook, S.A., Mestroni, L., Seidman, J.G., Seidman, C.E., 2012. Truncations of Titin Causing Dilated Cardiomyopathy. New England Journal of Medicine 366, 619-628.

Hoit, B.D., 2011. Strain and Strain Rate Echocardiography and Coronary Artery Disease. Circulation: Cardiovascular Imaging 4, 179-190.

Jawad, H., Ali, N.N., Lyon, A.R., Chen, Q.Z., Harding, S.E., Boccaccini, A.R., 2007. Myocardial tissue engineering: a review. Journal of tissue engineering and regenerative medicine 1, 327-342.

Jawad, H., Lyon, A.R., Harding, S.E., Ali, N.N., Boccaccini, A.R., 2008. Myocardial tissue engineering. Br Med Bull 87, 31-47.
Kitamura, H., Ohnishi, Y., Yoshida, A., Okajima, K., Azumi, H., Ishida, A., Galeano, E.J., Kubo, S., Hayashi, Y., Itoh, H., Yokoyama, M., 2002. Heterogeneous Loss of Connexin43 Protein in Nonischemic Dilated Cardiomyopathy with Ventricular Tachycardia. Journal of Cardiovascular Electrophysiology 13, 865-870.
Koch-Schneidemann, S., Gehr, P., Rutishauser, B., Eppenberger, H.M., 1994. Attachment of adult rat cardiomyocytes (ARC) on laminin and two laminin fragments. J Struct Biol 113, 107-116.
Maitra, N., Flink, I.L., Bahl, J.J., Morkin, E., 2000. Expression of alpha and beta integrins during terminal differentiation of cardiomyocytes. Cardiovascular research 47, 715-725.
Marian, A.J., Roberts, R., 1994. Molecular basis of hypertrophic and dilated cardiomyopathy. Texas Heart Institute Journal 21, 6-15.
Michel, J.B., 2003. Anoikis in the cardiovascular system: known and unknown extracellular mediators. Arterioscler Thromb Vasc Biol 23, 2146-2154.
Miskon, A., Ehashi, T., Mahara, A., Uyama, H., Yamaoka, T., 2009. Beating behavior of primary neonatal cardiomyocytes and cardiac-differentiated P19.CL6 cells on different extracellular matrix components. J Artif Organs 12, 111-117.
Morita, H., Seidman, J., Seidman, C.E., 2005. Genetic causes of human heart failure. The Journal of clinical investigation 115, 518-526.
Nguyen, M.-D., Tinney, J.P., Yuan, F., Roussel, T.J., El-Baz, A., Giridharan, G., Keller, B.B., Sethu, P., 2013a. Cardiac Cell Culture Model (CCCM) as a Left Ventricle Mimic for Cardiac Tissue Generation. Analytical chemistry 85, 10.1021/ac401910d.
Nguyen, M.-D., Tinney, J.P., Yuan, F., Roussel, T.J., El-Baz, A., Giridharan, G., Keller, B.B., Sethu, P., 2013b. Cardiac Cell Culture Model As a Left Ventricle Mimic for Cardiac Tissue Generation. Analytical Chemistry 85, 8773-8779.
Okita, K., Matsumura, Y., Sato, Y., Okada, A., Morizane, A., Okamoto, S., Hong, H., Nakagawa, M., Tanabe, K., Tezuka, K., Shibata, T., Kunisada, T., Takahashi, M., Takahashi, J., Saji, H., Yamanaka, S., 2011. A more efficient method to generate integration-free human iPS cells. Nature methods 8, 409-412.
Palatinus, J.A., Rhett, J.M., Gourdie, R.G., 2012. The connexin43 carboxyl terminus and cardiac gap junction organization. Biochimica et biophysica acta 1818, 1831-1843.
Rajala, K., Pekkanen-Mattila, M., Aalto-Set, #228, #228, , K., 2011. Cardiac Differentiation of Pluripotent Stem Cells. Stem Cells International 2011.
Ross, R.S., Borg, T.K., 2001. Integrins and the myocardium. Circ Res 88, 1112-1119.
Ruan, J.-L., Tulloch, N.L., Saiget, M., Paige, S.L., Razumova, M.V., Regnier, M., Tung, K.C., Keller, G., Pabon, L., Reinecke, H., Murry, C.E., 2015. Mechanical Stress Promotes Maturation of Human Myocardium From Pluripotent Stem Cell-Derived Progenitors. Stem cells (Dayton, Ohio) 33, 2148-2157.
Schwartz, K., Carrier, L., Guicheney, P., Komajda, M., 1995. Molecular Basis of Familial Cardiomyopathies. Circulation 91, 532-540.
Sehnert, A.J., Huq, A., Weinstein, B.M., Walker, C., Fishman, M., Stainier, D.Y., 2002. Cardiac troponin T is essential in sarcomere assembly and cardiac contractility. Nature genetics 31, 106-110.
Severs, N.J., Bruce, A.F., Dupont, E., Rothery, S., 2008. Remodelling of gap junctions and connexin expression in diseased myocardium. Cardiovascular research 80, 9-19.
Shimko, V.F., Claycomb, W.C., 2008a. Effect of Mechanical Loading on Three-Dimensional Cultures of Embryonic Stem Cell-Derived Cardiomyocytes. Tissue engineering. Part A 14, 49-58.
Shimko, V.F., Claycomb, W.C., 2008b. Effect of mechanical loading on three-dimensional cultures of embryonic stem cell-derived cardiomyocytes. Tissue engineering. Part A 14, 49-58.

Simon, A.M., Goodenough, D.A., Paul, D.L., 1998. Mice lacking connexin40 have cardiac conduction abnormalities characteristic of atrioventricular block and bundle branch block. Current biology : CB 8, 295-298.

Sun, N., Yazawa, M., Liu, J., Han, L., Sanchez-Freire, V., Abilez, O.J., Navarrete, E.G., Hu, S., Wang, L., Lee, A., Pavlovic, A., Lin, S., Chen, R., Hajjar, R.J., Snyder, M.P., Dolmetsch, R.E., Butte, M.J., Ashley, E.A., Longaker, M.T., Robbins, R.C., Wu, J.C., 2012. Patient-specific induced pluripotent stem cells as a model for familial dilated cardiomyopathy. Science translational medicine 4, 130ra147.

Terracio, L., Rubin, K., Gullberg, D., Balog, E., Carver, W., Jyring, R., Borg, T.K., 1991. Expression of collagen binding integrins during cardiac development and hypertrophy. Circulation research 68, 734-744.

Wang, X., Chun, Y.W., Zhong, L., Chiusa, M., Balikov, D.A., Frist, A.Y., Lim, C.C., Maltais, S., Bellan, L., Hong, C.C., Sung, H.J., 2015. A temperature-sensitive, self-adhesive hydrogel to deliver iPSC-derived cardiomyocytes for heart repair. International Journal of Cardiology 190, 177-180.

Willecke, K., Eiberger, J., Degen, J., Eckardt, D., Romualdi, A., Guldenagel, M., Deutsch, U., Sohl, G., 2002. Structural and functional diversity of connexin genes in the mouse and human genome. Biological chemistry 383, 725-737.

Willott, R.H., Gomes, A.V., Chang, A.N., Parvatiyar, M.S., Pinto, J.R., Potter, J.D., 2010. Mutations in Troponin that cause HCM, DCM AND RCM: what can we learn about thin filament function? Journal of molecular and cellular cardiology 48, 882-892.

Yamamoto, K., Dang, Q.N., Maeda, Y., Huang, H., Kelly, R.A., Lee, R.T., 2001. Regulation of Cardiomyocyte Mechanotransduction by the Cardiac Cycle. Circulation 103, 1459-1464.

Yang, T., Chun, Y.W., Stroud, D.M., Mosley, J.D., Knollmann, B.C., Hong, C., Roden, D.M., 2014. Screening for Acute IKr Block Is Insufficient to Detect Torsades de Pointes Liability: Role of Late Sodium Current. Circulation 130, 224-234.

Zhang, J., Klos, M., Wilson, G.F., Herman, A.M., Lian, X., Raval, K.K., Barron, M.R., Hou, L., Soerens, A.G., Yu, J., Palecek, S.P., Lyons, G.E., Thomson, J.A., Herron, T.J., Jalife, J., Kamp, T.J., 2012. Extracellular matrix promotes highly efficient cardiac differentiation of human pluripotent stem cells: the matrix sandwich method. Circ Res 111, 1125-1136.

Figure Captions

Figure 1. (A) Top and side view of PDMS stretcher device. Arrow: stretching direction. (B) Force that cells experience/cm^2 in the stretcher device. Arrow: 150 kPa at 1 Hz and an approximate 5% strain.

Figure 2. Characterization of healthy and DCM iPSC-CMs by (A) flow cytometry for expression of cardiac Troponin T with corresponding health and DCM iPSC-CM sheets (scale bars are 100 μm) and (B) immunostaining for expression of Troponin T and α-actinin. Evaluation of ECM coating materials under strain by (C) cell viability, (D) cell area, and (E) cell density of healthy iPSC-CMs. * $P<0.05$, † $P<0.01$, ‡ $P<0.001$, scale bars = 20μm

Figure 3. Expression of cardiac markers in healthy and DCM iPSC-CMs under different mechanical stimulation conditions. (A) TNNT2 gene, (B) MYL2 gene, (C) Cardiac Troponin T protein and (D) MLC-2v protein. Expression of these markers was highest in healthy iPSC-CMs under 5% static at the levels of both gene and protein. * $P<0.05$ vs. the line paired group; ‡ $P<0.05$ vs. the other test groups; ξ $P<0.05$ vs. the test groups of the same cell type.

Figure 4. Cell-cell interaction of healthy iPSC-CMs was increased by mechanical stimulation. (A) Immunofluorescence images of cardiac Troponin T expression in healthy and DCM iPSC-CMs under 5% static condition. Gene expression ratios (Healthy: Disease=H:D) of (B) connexin 43, (C) integrin alpha 5 (ITGA5), and integrin alpha 10 (ITGA10) in iPSC-CMs under each condition. Fold changes normalized by GAPDH. * $p<0.05$, comparison between healthy iPSC-CMs and DCM iPSC-CMs under the same mechanical stimulation. Scale bar = 200 μm. Dashed line at a fold change ratio of 1 in all plots.

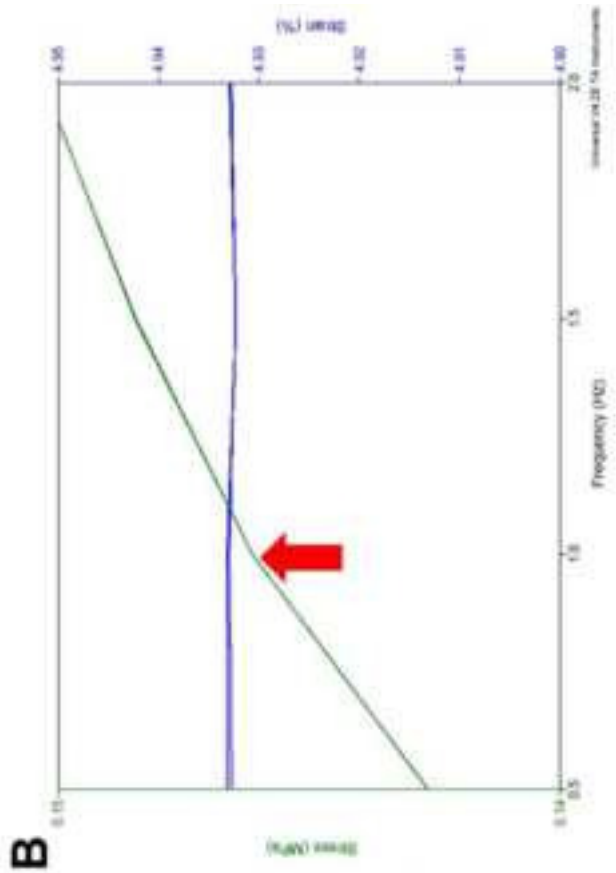

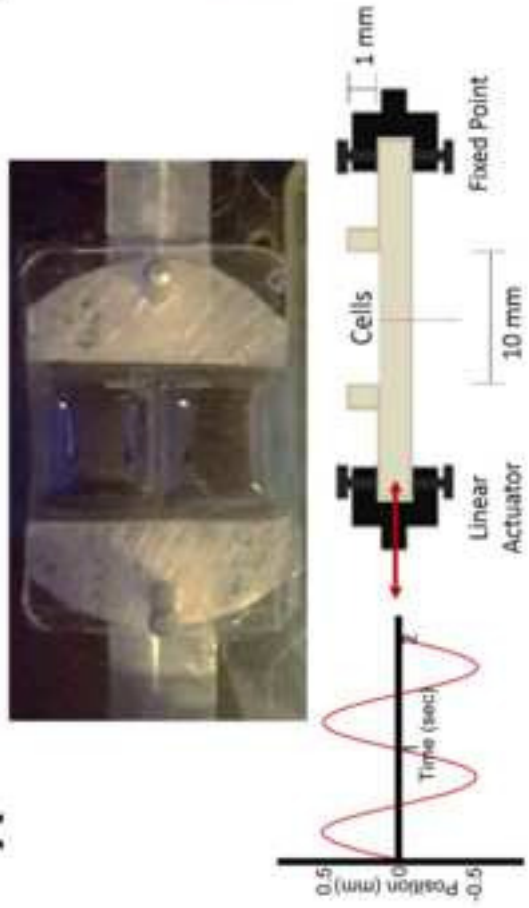

Figure. 1

Figure

Figure 2

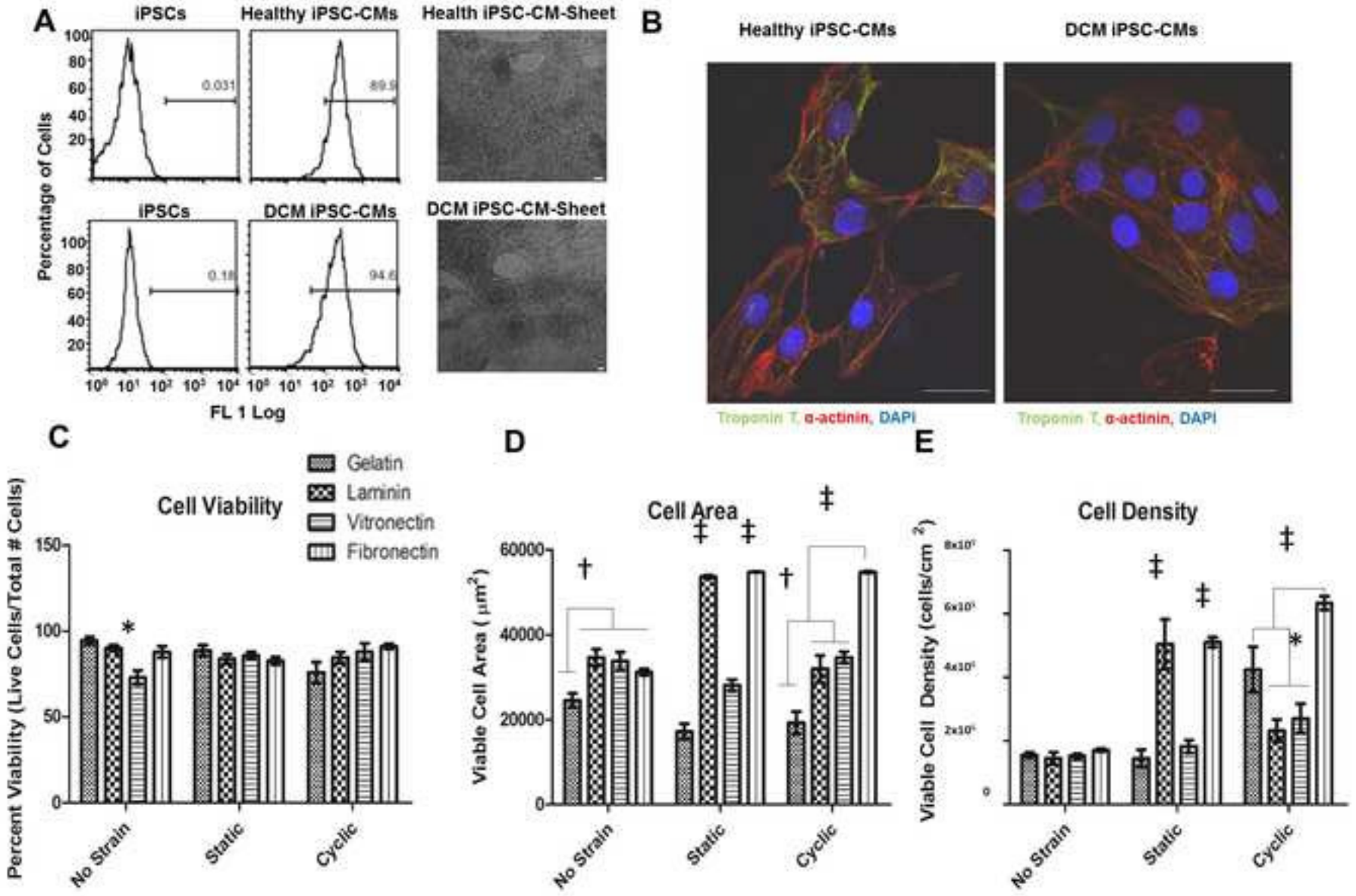

Figure 3

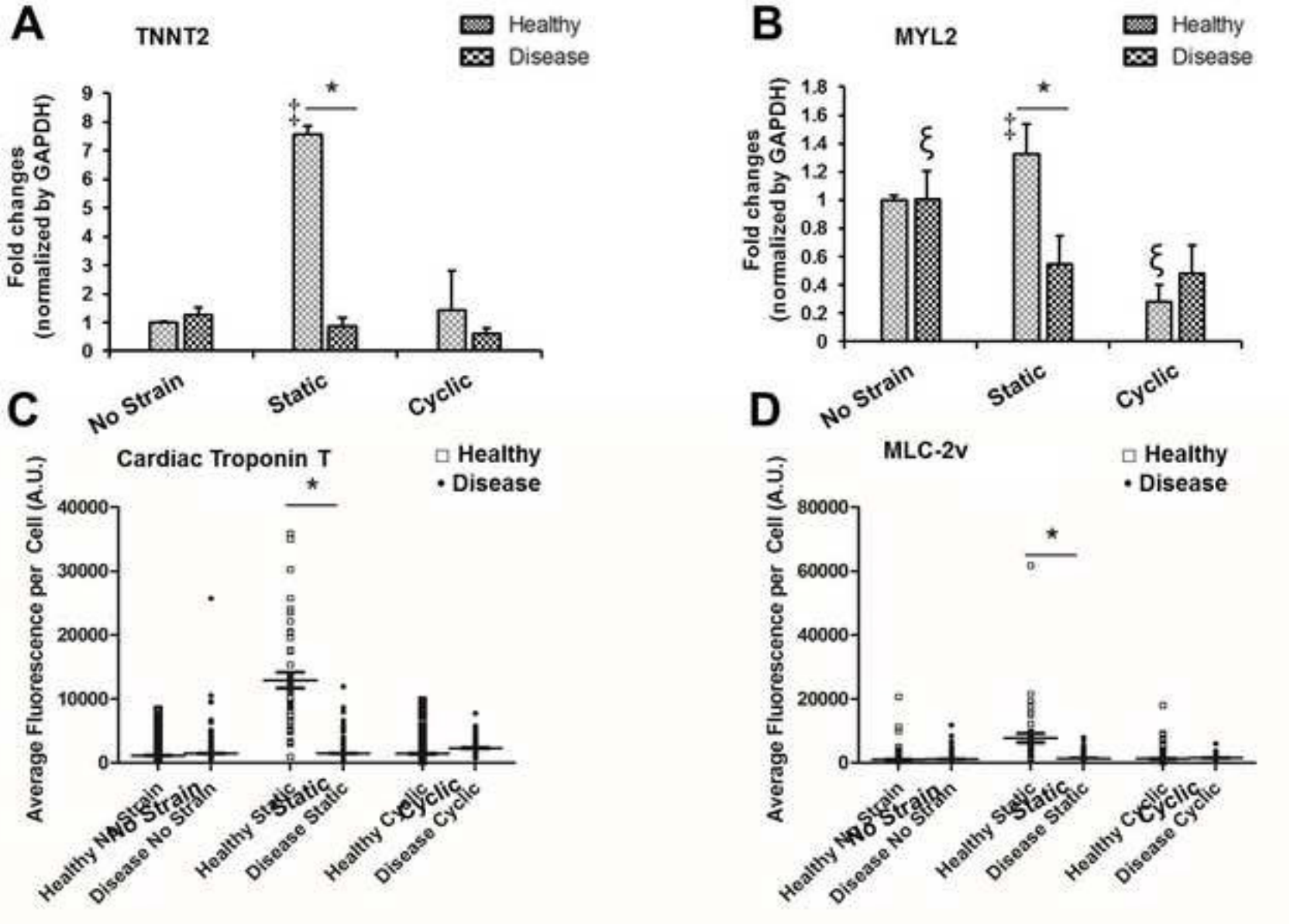

Figure 4